GEOPHYSICAL RESEARCH LETTERS, VOL. 27, NO. 18, PAGES 3021-3024, SEPTEMBER 15, 2000

Along strike variations in the electrical structure of the San Andreas Fault at Parkfield, California

Martyn Unsworth

University of Alberta, Edmonton, Alberta, Canada.

Paul Bedrosian

University of Washington, Seattle, Washington, U.S.A.

Markus Eisel, Gary Egbert and Weerachai Siripunvaraporn

Oregon State University, Corvallis, Oregon, U.S.A.

Abstract. Magnetotelluric exploration has been used to image along strike variations in the electrical resistivity structure of the San Andreas Fault at Parkfield, California. A low resistivity wedge extending to a depth of several kilometers is continuous over a horizontal distance of 8 km. The base of the wedge is coincident with the shallowest microearthquakes. A change in the electrical and fluid connection of the San Andreas Fault with a low resistivity zone in the Franciscan formation is observed along the Parkfield segment.

Introduction

Imaging the internal structure of active faults has advanced significantly in recent years. Seismic tomography has imaged both velocity contrasts across faults [*Eberhart-Phillips and Michael*, 1993] and a low velocity core within the fault [*Thurber et al.*, 1997]. Studies of trapped seismic waves have indicated the presence of a slow region in the core of the San Andreas Fault [*Li et al.*, 1997]. These observations are significant since low velocities may indicate the presence of fluids associated with the mechanics of earthquake rupture. Additional constraints on the nature of the fault core have come from magnetotelluric observations of the electrical resistivity of the San Andreas Fault at Parkfield and Carrizo Plain [*Unsworth et al.*, 1999]. In this paper we present additional magnetotelluric data that have imaged along strike variations in the structure of the San Andreas Fault at Parkfield.

Data acquisition

Magnetotelluric (MT) data were collected on three profiles that traversed the San Andreas Fault (SAF) on Middle Mountain in 1997 (Figure 1). Close to the fault, measurements were made every 100 m to provide a detailed image of the fault core. Further away data were recorded at more widely spaced sites. At each site the time series data were processed to yield estimates of apparent resistivity and phase from 100-0.001 Hz using the algorithm of *Egbert*, [1997]. Tensor decomposition was then applied to the data and showed that a two-dimensional (2-D) analysis was valid with a geoelectric strike approximately parallel to the San Andreas fault [*Chave and Smith*, 1994]. The data were then combined with the 1994 data, grouped into three profiles and inverted using the 2-D inversion scheme of *Mackie and Madden*, [1993]. These models fit data derived from both fault normal and fault parallel electric currents (the TM and TE modes respectively). Similar models were obtained with the inversion techniques of *Smith and Booker*, [1991] and *Siripunvaraporn and Egbert*, [2000]. In each inversion the data were fit with a root mean squared misfit of unity, generally within 10%. Owing to limited spatial coverage in certain areas, some sites were used in all three profiles. Thus only along-strike variations in structure within 8 km of the fault zone can be considered significant.

Each model shows a conductive zone coincident with the fault. To determine how deep this fault zone conductor (FZC) could extend, a second set of inversions were performed that started from a model with a very conductive fault zone. The inversion was continued until a misfit of unity was attained. These models are shown in Figure 2, and the depth extent of the shallower fault zone conductor is indicated by the black line.

Interpretation and discussion

West of the San Andreas Fault the Salinian granite is imaged on all three profiles with resistivities in excess of 300 Ωm. An offset in its top some 4 km west of the fault can be attributed to fault F2 (Figure 1). The average resistivity of the Salinian block appears to decrease slightly to the southeast.

The fault zone conductor on each profile is similar to that described by *Unsworth et al.*, [1999]. A range of depth extents for the FZC is consistent with the MT data (Figure 3). On Lines 1 and 0, a depth extent of 1.2 to 3 km is required by the magnetotelluric data. On Line 3 the conductor is better constrained with a range of 2.1 to 3 km.

Can the data distinguish between the deep and shallow FZC models? Two lines of evidence favor the deeper model. Firstly, while both deep and shallow models give the same overall fit to the data, the deep model gives a more uniform site-by-site misfit with the best fit at sites above the fault zone. Secondly, vertical magnetic fields were used to constrain the extent of the fault zone conductor. These data

Paper number 2000GL011476
0094-8276/00/2000GL011476$05.00

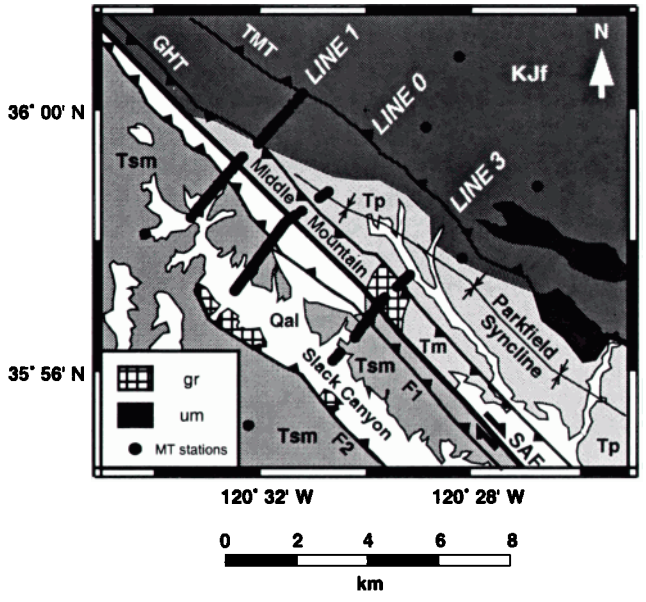

Figure 1. Simplified geological map based on *Dibblee* [1980], *Sims* [1990], *Hanna et al.*,[1972] and Mike Rymer (pers. comm., 1998). Qal = Quaternary alluvium; Tsm = Santa Margarita formation; Kjf = Franciscan formation, gr = Salinian granite and um = ultramafics, Tm,Tp = Great Valley formation. TMT = Table Mountain thrust fault and GHT = Gold Hill Thrust fault.

were not collected on Line 0 in 1994, but were recorded on Lines 1 and 3 in 1997. The data for Line 1 are displayed in Figure 4, along with the computed responses of the models with deep and shallow fault zone conductors. The vertical field data are not ideal, since they were only made every kilometer. However at 5 of the 7 measurement locations, it is clear that the deeper model gives the best fit to the observed data. On Line 3 the deep and shallow models are relatively similar and both are consistent with the vertical magnetic field data (which is noisier than on Line 1). The deeper FZC is the preferred model for Lines 1 and 0. Thus the FZC has a relatively constant depth extent along this segment of the San Andreas fault. On each profile it is bounded on its east side by the creep-defined surface trace (C) of the San Andreas Fault, and on the west by a thrust fault (F1).

East of the San Andreas Fault the geology is characterized by the Franciscan formation, overlain by Tertiary sedimentary rocks. On Line 3 these sedimentary units comprise the Parkfield syncline, some 2 km of the SAF. Here a low resistivity zone at the base of the syncline may be due to the presence of brines [*Jongmans et al.*, 1995]. To the northwest the Parkfield syncline shallows and coalesces with the San Andreas Fault. Thus on Lines 1 and 0 the syncline is not obvious and the shallow structure east of the SAF is dominated by westward dipping thrust faults (Mike Rymer, personal comm., 1998)

Further east on all lines is a larger zone of upper crustal low resistivity that extends to a depth of around 4 km within the Franciscan formation. This was first described by *Eberhart-Phillips and Michael*, [1993] who attributed coincident low resistivities and seismic velocities to the presence of brines. Assuming that these brines have the same salinity as observed in the Varian Well [*Jongmans et al.*, 1995], a porosity in the range 8-30 % is required by Archie's Law to explain this low resistivity. The increase in resistivity below 4 km does not imply the absence of fluids. Rather, it implies that increasing confining pressures reduce the porosity of the rock and the pathways available for electric current flow. To the northwest, the zone of low electrical resistivity approaches the San Andreas Fault, following the trend of the surficial geology (Figure 1).

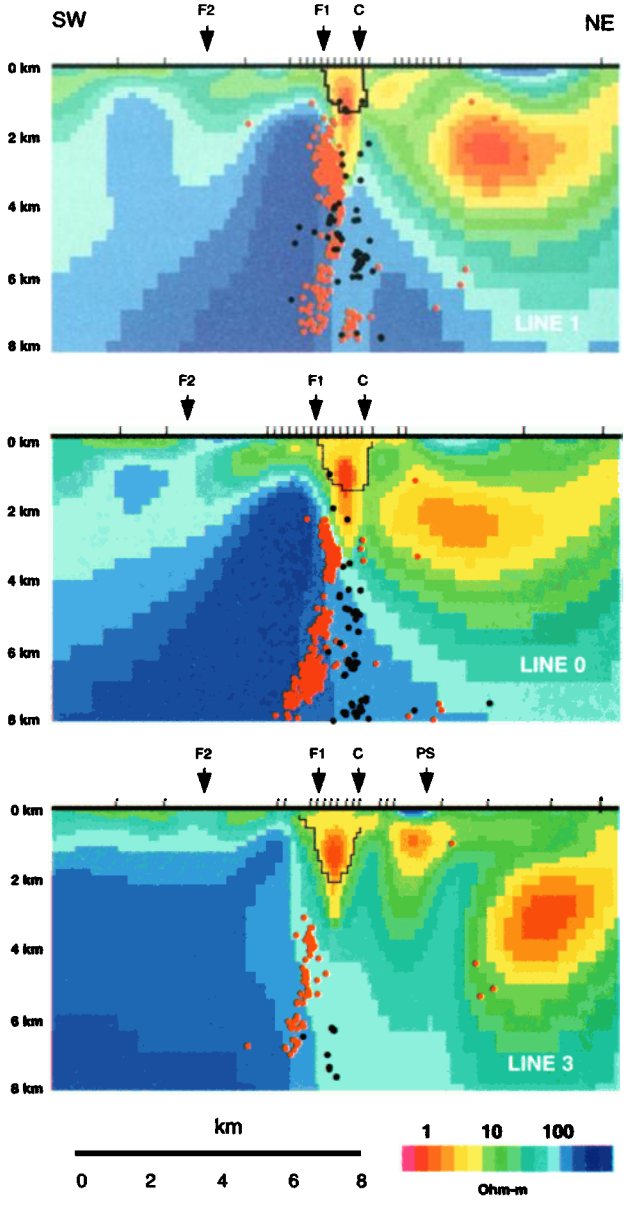

Figure 2. Electrical resistivity models for the three Middle Mountains profiles with the deep fault zone conductor. Earthquake hypocenters within 2 km of each profile are also shown. Red events are from the Parkfield High Resolution Network [*Nadeau and McEvilly*, 1997] and the black NCSN events were relocated by *Waldhauser and Ellsworth*, [1999]. Locations at which MT data were collected are indicated by vertical ticks. All models are shown with no vertical exageration. The black line indicates the 6 Ωm contour for models with a shallow fault zone conductor. C = surface trace of the San Andreas Fault defined by creep. PS = Parkfield Syncline.

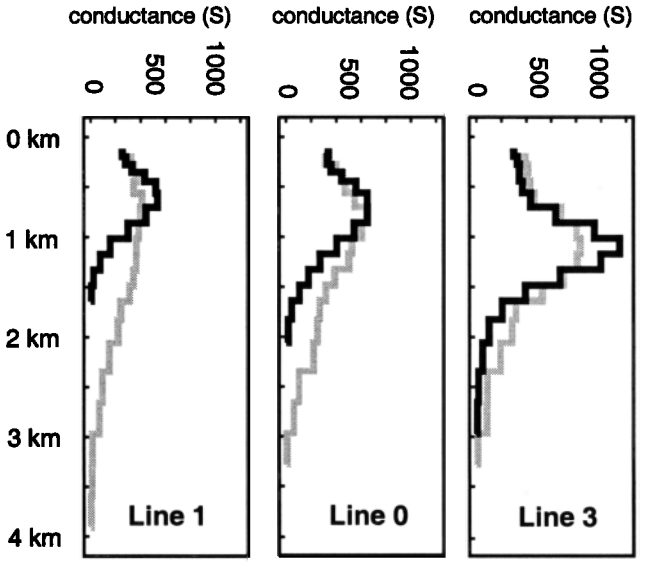

Figure 3. Variation of horizontally integrated conductance of the fault zone conductor as a function of depth. For each profile, both deep (grey) and shallow (black) models fit the data with an r.m.s. misfit of unity. The integration extends from the 30 Ωm contour on each side of the fault zone conductor.

Discussion and local seismicity

Figure 2 shows earthquake hypocenters within 2 km of each MT profile from the Parkfield High Resolution Seismic Network (HRSN) data of *Nadeau and McEvilly*, [1997] and the Northern California Seismic Network (NCSN) relocated by *Waldhauser and Ellsworth*, [1999]. The two patterns of seismicity are not completely consistent, but both are shown since each exhibits important features. The HRSN catalog contains many events with magnitudes less than M=2. The fault zone conductor is continuous along-strike and to first order its base is coincident with the depth at which the micro earthquakes begin. This might be expected if the FZC is composed of fluid saturated breccia that is too weak to accumulate stress and generate earthquakes. In this region, porosities in the range 8-30 % are required to account for the observed electrical resistivity. As clay minerals can lower electrical resistivity, these porosity values should be considered upper bounds.

The reduction in seismicity to the south east appears to be correlated with the increasing distance between the San Andreas Fault and the conductive zone within the Franciscan formation. This would be significant, since it has been suggested that fault creep (and associated microseismicity) on the San Andreas Fault is controlled by the availability of fluids coming from metamorphic reactions within the Franciscan [*Irwin and Barnes*, 1975]. Do the resistivity models in Figure 2 provide support for this scenario? Lines 1 and 0 exhibit abundant shallow seismicity and the characteristic M=6 events. The electrical resistivity structure shows a continuous low resistivity pathway to the east. In contrast, Line 3 has minimal shallow seismicity and the low resistivity zone in the Franciscan is spatially discontinuous due to a series of faults. This might imply a reduced fluid supply to the San Andreas fault on Line 3. Together, these observations suggest a mechanism for a connection between San Andreas seismicity and fluid structure within the Franciscan. However the structure of the San Andreas Fault at this location is complex (including a 5° bend at the Parkfield asperity). Further data acquisition and analysis are needed to fully image the 3-D electrical resistivity structure of this region and trace the hydrogeologic pathways.

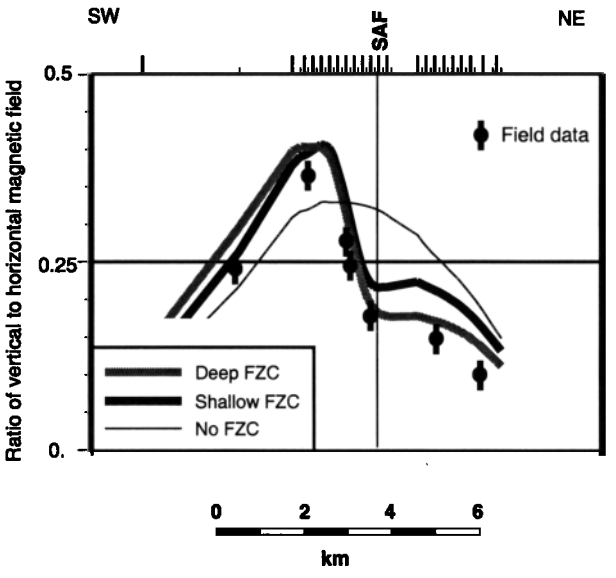

Figure 4. Ratio of vertical (H_z) and horizontal (H_h) magnetic fields, $T = |H_z/H_h|$ on Line 1 at a frequency of 0.1 Hz. The computed response of the shallow and deep FZC models are also shown. Note that the FZC increases T to the west of the fault and decreases it to the east.

Acknowledgments. This study was supported by the US Department of Energy Grant DE EG03-97ER-14781, NSF grant EAR9614411 and USGS grants 1434-HQ-97-GR-03157 and 1434-HQ-97-GR-03152. Fieldwork was made possible by the Parkfield landowners who generously allowed access to their property. Enthusiastic field help was given by Heidi Anderson, Sierra Boyd, Julian Douglass, Darcy Karakelian, Shenghui Li, Larissa Mitiagova, Lisa Stuebing, Neill Symmons, Handong Tan and Brad Wakoff. Ted Asch and Nestor Cuevas gave invaluable technical assistance. John Booker and Randy Mackie are thanked for the use of their inversion algorithms. Comments by an anonymous reviewer improved this paper.

References

Chave, A.D., and J.T. Smith, On electric and magnetic galvanic distortion tensor decompositions, *J. Geophys. Res., 99,* 4669-4682, 1994.

Dibblee, T. R., Geology along the San Andreas fault from Gilroy to Parkfield: in, Streitz, R. and Sherburne, R., eds., Studies of the San Andreas Fault Zone in Northern California, California Division of Mines and Geology, Sacramento, Special Report 140, p. 3-18, 1980.

Eberhart-Phillips, D., and A.J. Michael, Three-dimensional velocity structure, Seismicity and Fault Structure in the Parkfield Region, Central California, *J. Geophys. Res., 98,* 15737-15758, 1993.

Egbert, G.D., Robust multiple station magnetotelluric data processing, *Geophys. J. Int., 130,* 475-496, 1997.

Hanna, W. F., S.H. Burch, T.W. Dibblee, Gravity, magnetics and geology of the San Andreas Fault area near Cholame, California: U.S. Geological Survey Professional Paper 646-C, 1972.

Irwin, W.P., and I. Barnes, Effect of geologic structure and metamorphic fluids on seismic behavior of the San Andreas fault system in Central and Northern California: *Geology, 3,* 713-716, 1975.

Jongmans, D,. and P.E. Malin, Microearthquake S-wave Observations from 0 to 1 km in the Varian Well at Parkfield, California: *Bul. Seismol. Soc. Am. 85*, 1805-1821, 1995.

Li, Y., W.L. Ellsworth, C.H. Thurber, P.E. Malin and K. Aki, Fault-zone guided waves from explosions in the San Andreas Fault at Parkfield and Cienega Valley, California, *Bul. Seismol. Soc. Am., 87*, 210-221, 1997.

Nadeau, R., and T.V. McEvilly, Seismological studies at Parkfield V: Microearthquake sequences as Fault-zone drilling targets, *Bul. Seismol. Soc. Am., 87*, 1463-1472, 1997.

Mackie, R.L. and T.R. Madden, Three-dimensional magnetotelluric inversion using conjugate gradients, *Geophys. J. Int., 115*, 215-229, 1993.

Smith, J. T., and J. R. Booker, Rapid inversion of two- and three-dimensional magnetotelluric data, *J. Geophys. Res., 96*, 3905-3922, 1991.

Sims, J.D., Geologic map of the San Andreas fault in the Parkfield, 7.5-minute quadrangle, California: U.S. Geological Survey Miscellaneous Field Studies Map, MF-2115, scale 1:24,000, 1 sheet, 1990.

Siripunvaraporn, W., and G. Egbert, REBOCC: An efficient data-subspace inversion for two-dimensional magnetotelluric data, *Geophysics, 65*, 791-803, 2000.

Thurber, C.H., S. Roecker, W.L. Ellsworth, Y. Chen, W. Lutter and R. Sessions, Two-dimensional seismic image of the San Andreas fault in the Northern Gabilan Range, central California: evidence for fluids in the fault zone, *Geophys. Res. Lett., 24*, 1591-1594, 1997.

Unsworth, M.J., G.D. Egbert and J.R. Booker, High Resolution electromagnetic imaging of the San Andreas fault in Central California, *J. Geophys. Res., 104*, 1131-1150, 1999.

Waldhauser, F. and W.L. Ellsworth, A double difference earthquake location algorithm : Method and Application to the San Andreas and Hayward Faults, California, *Eos Trans. AGU, 46*, F705, 1999.

M.J. Unsworth, Department of Physics, University of Alberta, Edmonton, Alberta, T6G 2J1, CANADA. (unsworth@phys.UAlberta.ca)

P.A. Bedrosian, Geophysics Program, Box 351650, University of Washington, Seattle, WA 98195-1650, U.S.A.

M. Eisel, W. Siripunvaraporn and G.D. Egbert, College of Ocean and Atmospheric Sciences, Oregon State University, Corvallis, OR 97331-5503, U.S.A.

(Received February 7, 2000; revised June 28, 2000; accepted July 17, 2000.)